J. Anat. (1995) 187, pp. 547–562, with 10 figures Printed in Great Britain

Segregation and convergence of specialised pathways in macaque monkey visual cortex

S. SHIPP AND S. ZEKI

Department of Anatomy, University College, London, UK

(*Accepted 13 June 1995*)

ABSTRACT

At the level of cortical area V2, the various visual inputs to the cortex have reorganised to form 3 distinct channels. Anatomically these are embodied in the thick and thin dark stripes, and paler interstripes characteristic of cytochrome oxidase architecture. Do the outputs of these compartments remain segregated at higher levels of processing, or are they in turn combined and repackaged? To examine this question we have injected distinct orthograde tracers into the functionally distinct areas V4 and V5 of one hemisphere in 3 macaque monkeys (*Macaca fascicularis*). V4 is known to receive input from both thin stripes and interstripes of V2, but some parts of V4 receive only interstripe afferents, others receive a relatively greater contribution from the thin stripes. Thus V4 itself is thought to possess subcompartments of at least two distinct types, acting to extend the blob-thin stripe and interblob-interstripe pathways through V1 and V2. The experiments reported here reveal no further divergence between these channels: both types of V4 subcompartment make rather similar patterns of connection with further visual areas and subcortical structures. In contrast to V4, area V5 receives input from the thick stripes of V2. V4 and V5 are weakly interconnected, at best, and there is limited direct convergence in their two sets of ascending connections. For instance, both areas send output to area LIP; but V4 targets the dorsal half of the area, and V5 the ventral half, with some minor overlap. Projections to the superior temporal sulcus are also mainly separate, although we found instances of direct convergence in areas FST and possibly V4t. Segregation is also the rule for subcortical connections to the pulvinar from these two areas. In summary, the segregated outputs of V2 can remain largely distinct through at least two subsequent stages of cortical processing.

Key words: V4; V5; LIP; inferior pulvinar; cytox stripes; parallel pathways

INTRODUCTION

At its outset, the visual system has three major constituents, deriving from the Pα, Pβ and Pχ ganglion cells of the retina (Shapley & Perry 1986). The former pair segregate into the M (magnetocellular) and P (parvocellular) layers of the lateral geniculate nucleus (LGN) (Perry et al. 1984), whose subsequent contribution to the central visual pathways has become the subject of close scrutiny. Initial descriptions of the relay of M and P signals through V1 suggested a high degree of independence. Subsequent analysis of their progress through prestriate cortex gave rise to the speculation that all visual capacities, and all visual cortex, could be divided into two domains, one M dominated and one P dominated (Livingstone & Hubel, 1984, 1987*a*, *b*). Latterly this notion has been undermined by observations that reveal the anatomical potential for mixing between the M and P streams in V1 (Lachica et al. 1992; Yoshioka et al. 1984) and physiological confirmation of this fact (Nealey & Maunsell, 1994); there is also the contribution from the third pathway to consider (Perry & Cowey 1984; Hendry & Yoshioka, 1994). One analogous possibility, however, is that V1 remixes its three input channels into three new output channels, two of which find anatomical expression in the blobs and interblobs of layers 2 and 3 while the

Correspondence to Dr S. Shipp and Prof. S. Zeki, Department of Anatomy, University College London, Gower Street, London WC1E 6BT, UK.

third evolves in layer 4B. The thin stripe, interstripe and thick stripe compartments of V2 can be regarded as the immediate extension of these channels from V1 into prestriate cortex (Livingstone & Hubel, 1984, 1987*a*). The question addressed here is whether these three pathways emanating from V2 continue to show signs of anatomical segregation at subsequent stages of cortical processing, or whether they too re-amalgamate and lose their identity.

The method we adopted was to examine the connections of two areas already known to receive separate inputs from V2, namely areas V4 and V5 (Zeki, 1971). V5 receives input almost exclusively from the thick stripes of V2 (DeYoe & Van Essen, 1985; Shipp & Zeki, 1985, 1989*b*). V4, by contrast, forms the extension of both the blob-thin stripe and interblob-interstripe pathways (DeYoe & Van Essen, 1985; Shipp & Zeki, 1985; Nakamura et al. 1993). But the latter two pathways seem to retain their separate identities within V4, in subcompartments that we refer to as type I and type II respectively, although the specific modular substructure of V4 has yet to be determined (Zeki & Shipp, 1989; Van Essen et al. 1990). We placed distinct orthograde neural tracers into V4 and V5 in each of 3 hemispheres in order to reveal subsequent targets of these pathways and, more importantly, to reveal any direct overlap between them. We used tritiated amino acids in V5, and HRP-WGA in V4; the latter, being a bidirectional tracer, also reveals whether the thin stripes or interstripes are the principal source of the input from V2. Thus we were able to distinguish the connection of type I and type II compartments in V4, in order to compare the further distribution of each with the other, as well as with that of V5.

METHODS

We used a cocktail of tritiated amino acids (TAA)-L[5-^{3}H]proline (33Ci/mmol) and L-[4,5-^{3}H]leucine (186 Ci/mmol) (Amersham), reconstituted to yield an equimolar mixture with radioactive concentration 300 μCi/μl. The HRP-WGA (Sigma) was a 4% solution in deionised water. Monkeys SP40 and SP42 received multiple injections into both areas (up to 0.5 μl of WGA-HRP total in V4 and 0.8 μl of the cocktail in V5); the third monkey, case SP43, received single injections of 0.06 μl WGA-HRP and 0.5 μl of the cocktail. V4 was injected over the surface and posterior bank of the prelunate gyrus, where we expected to find a representation of the central 10° of the inferior contralateral quadrant (Maguire & Baizer, 1984; Gattass et al. 1988). The injections in V5 were aimed at a topographically equivalent region, identified by prior physiological recordings; the headstage assembly was then replaced in the micromanipulator by the injection syringe, the syringe tip placed over the observed site of electrode entry and driven at the same angle to the same depth (Shipp & Zeki, 1989*a*). The adequacy of this procedure was subsequently checked by examination of the topographic distribution of transported label in V2, whose visual topography is well established (Gattass et al. 1981). The monkeys were given a lethal overdose of anaesthetic and perfused within 3–4 days of tracer injection. One to two weeks earlier we had also transected the splenium of the corpus callosum of each animal, in order to afford the pattern of interhemispheric connections by later staining for axonal degeneration.

The brains were processed by standard methods, described previously (Shipp & Zeki, 1989*a*, *b*). Briefly, the occipital operculum was removed, flattened and sectioned tangentially, to generate sections passing roughly parallel to the layering of V2 in the posterior banks of the inferior occipital and lunate sulci. The remainder of the brain was cut horizontally, in a sequence 60/60/30/60/30/30 μm. A 1-in-3 set of 60 μm sections was reacted for HRP-WGA using tetramethyl benzidine (TMB) as the chromogen (Mesulam, 1982); alternate sections were subsequently counterstained with cresyl violet. A 1-in-6 set of contiguous sections was processed for autoradiography (Cowan et al. 1972). A minority of sections were treated by both procedures (but using the more stable diamino benzidine (DAB) as a peroxidase chromogen) in order to confirm any overlapping projections more directly. A further 1-in-3 set of 30 μm horizontal sections was stained for callosal axon degeneration (Fink & Heimer, 1967). The operculum was cut uniformly at 50 μm and sections processed alternately for cytochrome oxidase (Wong-Riley, 1979), HRP-WGA and autoradiography, as above. Stained sections were drawn under cross-polarising optics (WGA-HRP), dark field (TAA) or bright field (degeneration). The essential feature of the procedure is to compile the presence and density of each label onto a single contour line, drawn through layer 4. Densities were classified as zero or positive grades 1–4. We drew the outlines of the HRP-WGA sections first, and superimposed on these the label densities from the autoradiographs and degeneration stains. The former sections undergo the greatest shrinkage, but are less flimsy and less prone to distort when mounted onto glass slides. The digitised contours through layer 4, bearing all three sets of label densities as well as

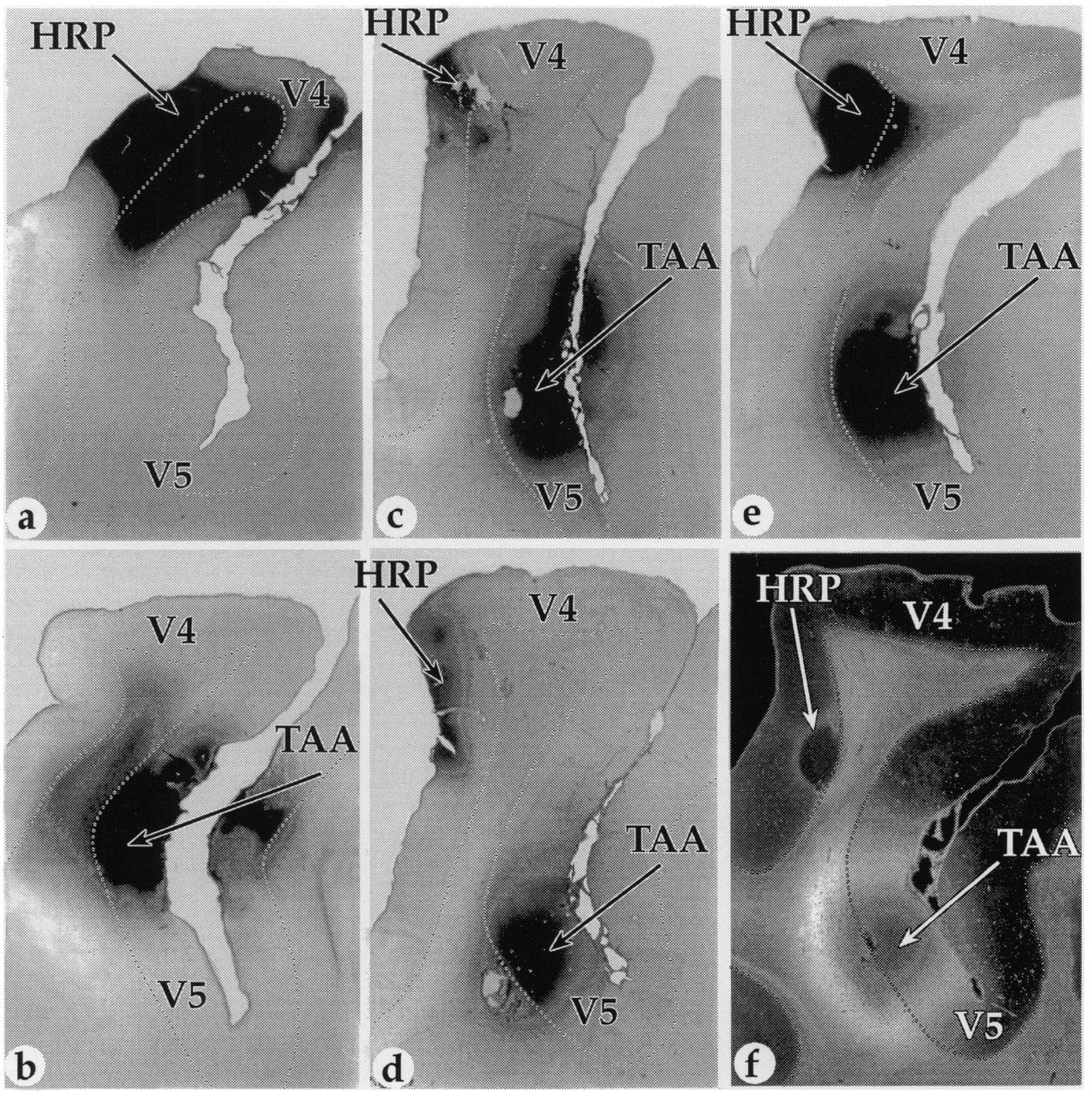

Fig. 1. Photomicrographs to illustrate the injection sites (HRP-WGA into the posterior prelunate gyrus and TAA into the posterior bank or fundus of the superior temporal sulcus) in each case: (*a*), (*b*) SP40; (*c*), (*d*) SP42; (*e*), (*f*) SP43. These are horizontal sections from which the posterior bank of the lunate sulcus (part of the occipital operculum) has been removed; anterior is to the right and lateral to the top. The upper row of sections is taken from a more dorsal level than the bottom row and the level of each section is also indicated on the reconstructions of the superior temporal sulcus in Figure 9. (*a*) to (*e*) are brightfield illumination; (*f*) is darkfield and shows the typical sizes of the TAA 'core' and 'halo'. The HRP-WGA injection sites are stained using DAB as the chromogen, whose reaction product is more restricted than that obtained using TMB.

markers for anatomical features, are the raw material for computer-aided reconstructions. We use both 3D and 2D methods, employing purpose-written software (Romaya & Zeki, 1985; Shipp & Zeki, 1989*a*). The former is naturally superior for rendering a recognisable image of the cortex. The contour lines are presented as a wireframe model with hidden line removal, sectors occupied by label being brightened and/or coded chromatically. We use the 2D method to reconstruct individual gyri and sulci, within which the distortion inherent in flattening is minimal despite the contour lines being made fully linear. The 2D format also allows for a more subtle rendition of variation in the density of labelling, as random dot patterns expanded orthogonal to the axis of the straightened contour lines.

RESULTS

Injection sites

Although 4 of the 6 injection sites were of a composite nature, none showed a nonuniform deposition of tracer. Each site is illustrated by photomicrographs in Figure 1. The V4 injection in SP40 was the largest, spreading into both banks of the prelunate gyrus. It was also the most dorsally located, and may thus have spread into area DP, whose border with V4 is poorly defined. The other 2 injections of HRP-WGA were centred more posteriorly on the gyrus (i.e. in the anterior bank of the LS) and were unlikely to have exceeded the bounds of V4. The TAA injections into V5 were precisely located deep in the posterior bank of the STS, but each also showed some sign of leakage onto the anterior bank of the STS on insertion/withdrawal of the syringe. Only in the first case (SP40) did the density of silver grains on the anterior bank (likely area V5A/MST) seem substantial enough to have contributed, possibly, to the observed patterns of transport. We subdivided all injections into 'core' and flanking 'halo' regions. The significance of the latter is that it may, possibly, obscure lighter connections/weaker labelling from the same tracer—but as there was no sign of any cross-reactivity in our staining procedures, the TAA halos had no effect on the detection of HRP-WGA transport, or vice versa.

Distribution of label in V2

As expected, all 3 injections into V4 produced label within the posterior bank of the LS, a part of V2 representing the inferior contralateral visual field. By comparing the distributions of labelled cells to the cytochrome oxidase stripes in V2, cases SP40 and SP43 were classified as type I and SP42 as type II: types I and II refer to bands of labelled cells in V2 that are centred on the thin stripes and interstripes respectively; we also use the same terms to designate the two types of module that are implied to exist in V4. Thus the type I module in V4 is the likely extension of the blob-thin stripe pathway and the type II module is the likely extension of the interblob-interstripe pathway. These observations are fully described by Zeki & Shipp (1989) (see figs 4, 6 and 5 from that paper, respectively).

Figure 2 shows the type I distribution of V4 label found in the operculum of case SP43, together with the distribution of terminal TAA label demonstrating the feedback projection to V2 from V5. The latter is incident on the thick stripes, and so interdigitates between the bands of 'V4' label. (Other, more sensitive demonstrations of the back projection from V5 to V2 show that it also extends between the thick stripes, thus overlapping the territory connected to V4 (Shipp & Zeki, 1989*b*)). We drew outlines around the perimeter of both labelled regions and transferred them to a schematic chart of V2, as illustrated in Figure 3. This labelling was within the posterior bank of the lunate sulcus, a part of dorsal V2 that represents the central portion of the contralateral inferior quadrant. The superior quadrant occupies the matching chart of ventral V2 which, in case SP43 for instance, shows additional overlapping regions of V4 and V5 label; the latter were located posteriorly on the inferior temporal gyrus, a part of V2 external to the operculum that was reconstructed from conventional horizontal sections. We used these schematic charts of V2 as an index of the degree of visuotopic overlap between the 2 injections in each case. They are better regarded as maps of the visual field distorted to mimic the conformation of V2, than as physical maps of V2 in each individual (the regions shaded in grey approximate the cortex buried within a typical pattern of sulci). We deduce from the charts of V2 that the injection sites occupied at least partially overlapping

Fig. 2. Case SP43 showing the relative distribution of connections within area V2. Orthograde TAA label from V5 (cross hatching) and retrograde label from V4 (stipple) were drawn from an adjacent pair of tangential sections through the posterior bank of the lunate sulcus, and superimposed on the same diagram using blood vessels as local points of reference. Bar, 2 mm.

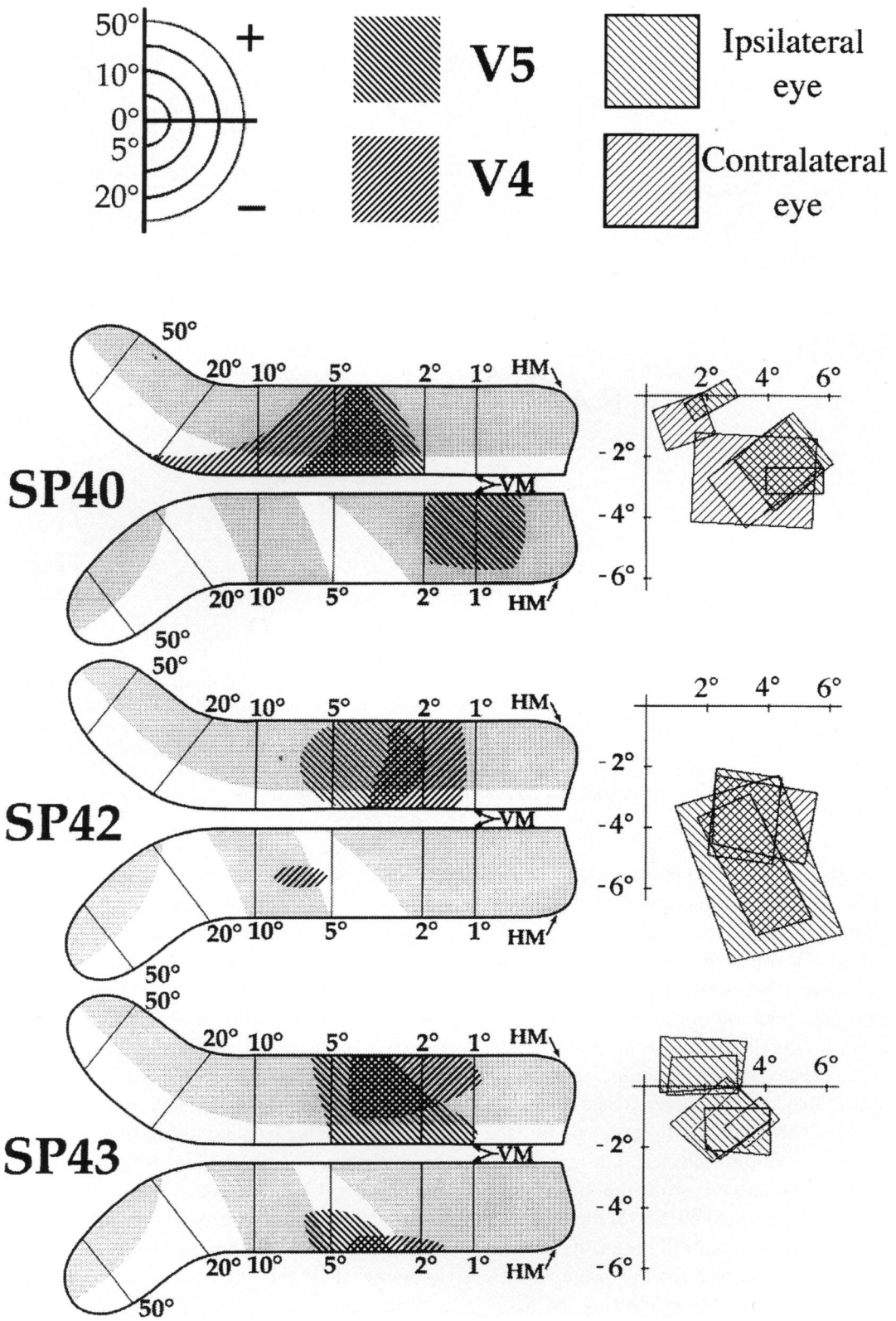

Fig. 3. Schematic maps of V2 to show the distribution of each tracer—and by implication the region of the visual map in V4 or V5 that was injected—in each of the 3 cases. The locations of the lines of isoeccentricity, and the shaded regions (which depict cortex buried within sulci) are intended only as rough guides, since the precise map and the conformation of sulci vary substantially between individuals. The upper part of each pair shows dorsal V2, which maps the contralateral inferior quadrant within the lunate and parieto-occipital sulci; the lower part of each pair shows ventral V2, which maps the contralateral superior quadrant within the inferior occipital, occipitotemporal and calcarine sulci. To the right of each anatomical map are shown receptive fields recorded at the first injection site in V5 (there were 3 TAA injections into V5 in SP40, and 2 in SP42, spaced about 1 mm apart).

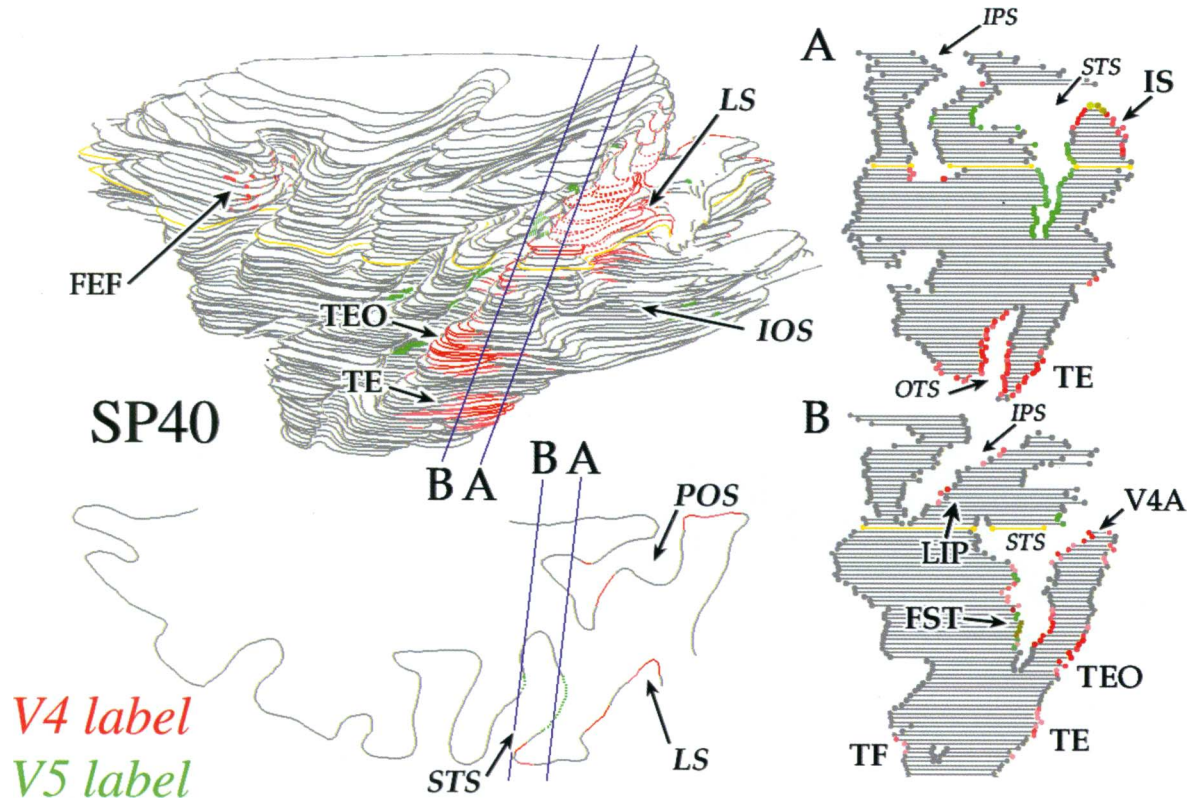

Fig. 4. 3D reconstruction of an injection of HRP-WGA into dorsal V4 (case SP40: type I), with horizontal and near-coronal slices (A, B) to show the distribution of connections (red). Projections from the TAA injection site in V5 (green) are all within sulci, and hence less visible on the surface view of the hemisphere. Straight blue lines mark the location of the coronal sections which are planar with the line of sight. The 3D contour corresponding to the isolated horizontal section is shown in yellow. The occipital operculum has been removed from the posterior end of the hemisphere (right) so that parts of the anterior banks of the lunate and inferior occipital sulci are now visible. The injection site is indicated by a region of broken lines on horizontal sections, and by 'IS' on the coronal sections. For explanation of abbreviations, see text.

zones in the maps of V4 and V5 in all 3 cases. Within V2, the area of overlap ranged from 25% to 50% of the area occupied by each label singly.

Shown to the right of each topographic chart are the receptive fields that were recorded from the vicinity of the corresponding injection site within V5. Since these RFs were obtained from a single site within the larger injected region (encompassing several mm^2 of cortex), they should cover a less extensive zone of visual field than that revealed by the anatomical survey of V2 for each case. The visual field plots are roughly congruent with the anatomical charts, although in 2 cases (SP40, SP43) the receptive fields seem to extend more centrally than the cortical disposition of label; to account for the discrepancy it may be noted that small errors in plotting the fovea may translate into several mm of cortex, given the high magnification factor of central V2 [about 10 mm deg^{-1} at $-1°$ on the inferior VM at the border with V1 (Tootell et al. 1988)].

In the third case, SP42, the autoradiographic procedure for the operculum sections was faulty, and a subsequent re-emulsioning procedure was also negative, so no V5-label was visualised in the central regions of V1 and V2 (approximately 0°–10° eccentricity). Because the residual, peripheral parts of V1 and V2 (examined in label-positive horizontal sections) were completely blank, we infer that the output to V1 and V2 from this V5 injection was all directed towards the compromised opercular tissue. The remainder of the visual cortex and subcortex showed a very typical labelling pattern for a V5 injection, and we have no doubt that the injection was correctly situated in V5. The distribution of V5-label within dorsal V2 that is shown for Fig. 3/SP42 was estimated from the distribution of label in dorsal V3; no V5-label was present in ventral V3 in this case, implying that the injection was restricted to the inferior quadrant of the map in V5. The receptive fields recorded from SP42 were sufficient to confirm a central location in the inferior contralateral quadrant.

Connections of V4

Two cases, SP42 and SP43 (type II and type I, respectively), had injections placed in near correspond-

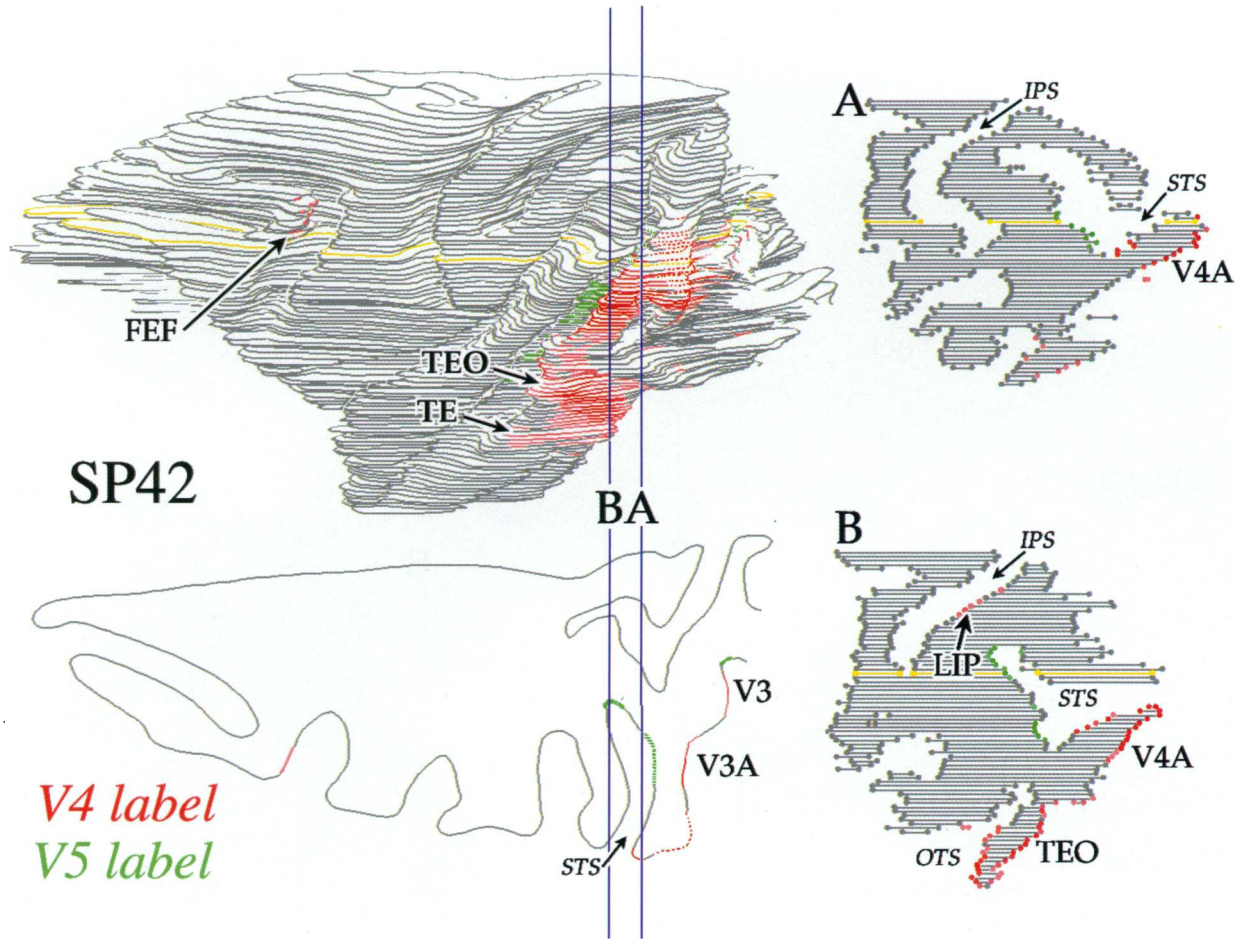

Fig. 5. 3D reconstruction of an injection of HRP-WGA into central V4 (case SP42: Type II) and of TAA into V5. Conventions as for Figure 4.

ing locations on the prelunate gyrus, roughly level with the tip of the LS. Their visual topography is much alike, in that both are centred around 2° eccentricity in the inferior visual field, although both also show some invasion of the superior quadrant. The third case, SP40, revealed no involvement of the superior visual field. This injection was placed more dorsally on the prelunate gyrus, and the label within V2 extended further medially into the parieto-occipital sulcus (POS), corresponding to a more eccentric sector of the inferior quadrant. These findings concur with existing topographic maps of V4 (Maguire & Baizer, 1984; Gattass et al. 1988).

The global pattern of connections of V4 in these cases is illustrated by 3D reconstructions of each hemisphere in Figures 4–6. The patterns of distribution of label are fundamentally similar. The most important observation, in the current context, is that there is no major difference that can be attributed to the type I or type II status of these 3 injections—and hence no evidence that the blob-thin stripe and interblob-interstripe pathways begin to diverge once they emerge from V4.

We focus upon the 'ascending' projections from V4, which represent the continuation of these pathways to still higher areas and which can be recognised by the concentration of terminal label within layer 4. There were strong ascending projections to multiple sites within the inferotemporal cortex (ITC), the superior temporal sulcus (STS), the intraparietal sulcus (IPC) and the arcuate sulcus (AS). The subdivision of most of these sites into separate areas is not well understood, so the accompanying terminology is somewhat provisional. The most extensive outputs from V4 were to ITC, including areas TEO and TE on the lateral surface and area TF on its ventral surface (going by the demarcations of Boussaoud et al. (1991) and Distler et al. (1993)). Equally dense was the output to a region directly adjacent to V4 on the anterior rim of the prelunate

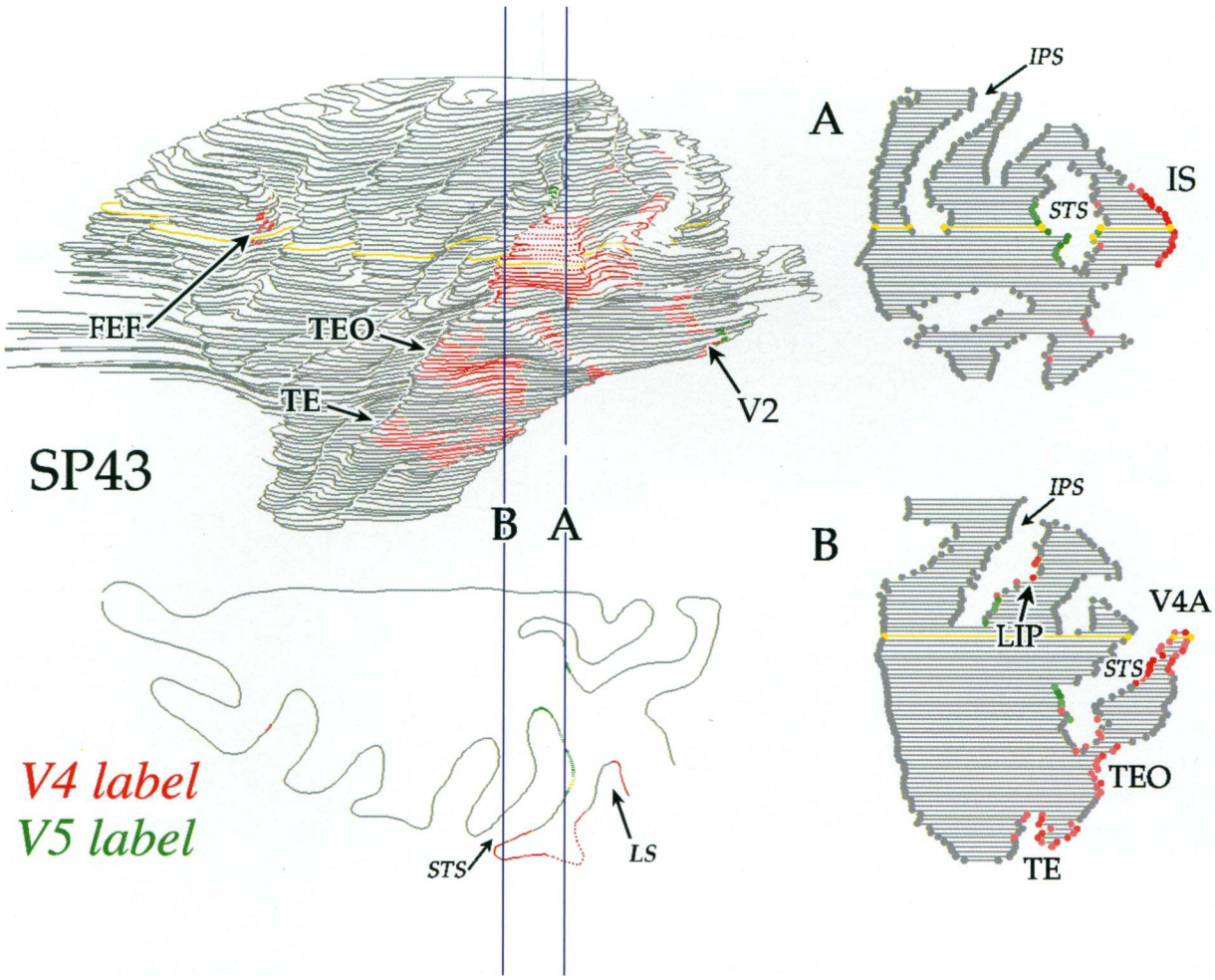

Fig. 6. 3D reconstruction of an injection of HRP-WGA into central V4 (case SP43: Type I) and of TAA into V5. Conventions as for Figure 4.

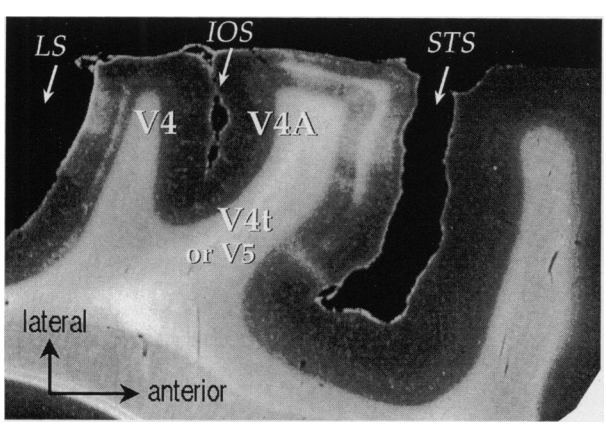

Fig. 7. Horizontal section from case SP42, taken at the level shown in Figure 9, reacted for WGA-HRP after an injection in area V4. Three types of connection, with distinctly different laminar labelling characteristics, are visible: an intrinsic connection within V4, an ascending connection to V4A, and an ascending/intermediate connection, probably area V4t.

gyrus, which also extends a few mm inside the STS (Fig. 7): we refer to this output zone as area V4A. Consistent projections were also found to area LIP in the IPS, and the frontal eye fields in the anterior bank of the AS. All these areas were labelled in all 3 cases, and we conclude that they each receive input from both type I and type II compartments in V4.

Also present were intermediate or descending connections to areas V3A and V3 in the LS, and to several sites in the POS, possibly areas V3A or PIP. Here again there was no evident distinction to be made between the type I and type II cases. The most notable difference, in fact, was between case SP40 (type I) and the others. The former had rather greater projections to sites more temporal than V4A within the STS, and more extensive connections with the IPS and POS. These differences could well reflect the placement of this injection at a site of greater eccentricity. It is also possible that the injection site

also involved part of the dorsal prelunate area (DP), a very poorly characterised zone lying immediately dorsal to V4. The latter possibility is one to bear in mind when considering the results of overlap in the output from V4 and V5, presented below. Both type I cases revealed a minor output to area DP, which we did not observe in case SP42 (type II) and this was the sole example that we could identify of a difference in connectivity that might be related to the modular organisation of V4.

'Juxtaconvergence' in the outputs of V4 and V5

The neologism refers to the fact that we found substantial outputs from these areas to nearby cortical and subcortical sites, but limited instances of direct overlap, at least in the ascending projections. Juxtaconvergence was observed within both the IPS and STS, and subcortically within the inferior pulvinar of the thalamus. We describe each in turn, below.

Lateral bank of the intraparietal sulcus. The basic observation here is that V4 projects mainly to the upper part of the lateral bank of the IPS, and V4 to the lower part (nearer to the fundus), as evident in all 3 reconstructions of the IPS in Figure 8. This is a general finding among many other single-injection cases of V4 or V5 which we have examined (but whose description exceeds the scope of this report). All of these outputs had the laminar pattern typical of ascending connections (Rockland & Pandya, 1979; Felleman & Van Essen, 1991), with a very evident concentration of terminal label in layer 4. There was modest overlap of the V4 and V5 projection domains in cases SP42 and SP43, and rather more in case SP40, where one heavy patch of HRP label was found at a greater than average depth within the sulcus. Another general feature is that both projections tend to terminate in bands that are oriented dorsoventrally, i.e. roughly orthogonal to the line of the fundus. It is notable that these banded projections from V4 and V5 tend to co-align with each other; furthermore, the reconstructions in Figure 8 show them to be coincident with similarly periodic bands of callosal label. These anatomical features introduce a transverse element to the functional architecture within the IPS, in contrast to existing descriptions which emphasise the longitudinal subdivision between areas VIP and LIP.

Area VIP was initially defined as the projection zone within the IPS of area V5 (Maunsell & Van Essen, 1983). However, area LIP, immediately dorsal to VIP, is also reported to connect with V5 (Andersen et al. 1990; Blatt et al. 1990). The border between these 2 areas has recently been localised physiologically (Colby et al. 1993), and reported to coincide with the existing myeloarchitectural demarcation; so defined, VIP and LIP both receive a projection from V5 (Ungerleider & Desimone, 1986). The VIP/LIP border could not be recovered from our material, but we note that it seems, in general, to be somewhat ventral to the dividing line between the V4 and V5 projection domains. This implies that area LIP, as currently defined, may be subdivided into a dorsal zone (LIPd) connected to V4, and a ventral zone (LIPv) connected to V5; LIPd and LIPv are also distinguishable in myelin stained tissue, since the former is reported to be more lightly myelinated (Blatt et al. 1990). Both subregions of LIP may also be constituted from discrete transverse compartments, as indicated by the periodicity of coincident intra and interhemispheric association connections.

An alternative hypothesis is that the disposition of the connections from V5 and V4 simply reflects the relative visuotopic locations of the injection sites in each case, in a manner that is determined by the nature of the retinal map in area LIP. Retinotopic order is not greatly preserved within area LIP, although some mapping data have been provided by Blatt et al. (1990). This map may be used to predict the relative arrangement of label in LIP according to the visuotopic placements of the injections in each case (as documented in Fig. 3), but the outcome bears scant correspondence to the patterns we actually observed. In general, the 'retinotopic hypothesis' seems inadequate because the consistency with which the V4 projection zone extends more dorsally than that of V5 is at odds with the case-to-case variation in relative topography of the injection sites.

Superior temporal sulcus. For convenience, the STS can be divided into its posterior bank, 'floor' and anterior bank. Most projections from V4 terminate in the posterior bank; projections from V5 were found mainly in the floor and anterior bank (Fig. 9). There were few instances of overlap, the most prevalent being within the fundus, ventral to the injection site in V5. This is possibly area FST of Desimone & Ungerleider (1986). Another site of overlap was a small zone just lateral (or posterior) to V5, which might correspond to area V4t (Maguire & Baizer, 1984; Desimone & Ungerleider, 1986).

Of the projections from V4, the most dorsal concentration (sited on the posterior lip of the sulcus and the adjoining gyral surface) is V4A, as mentioned above. Just adjacent to V4A within the STS, and recognisable by the fact that terminal label was less concentrated within layer 4, was a small patch of label that might correspond to area V4t (see Fig. 7). A

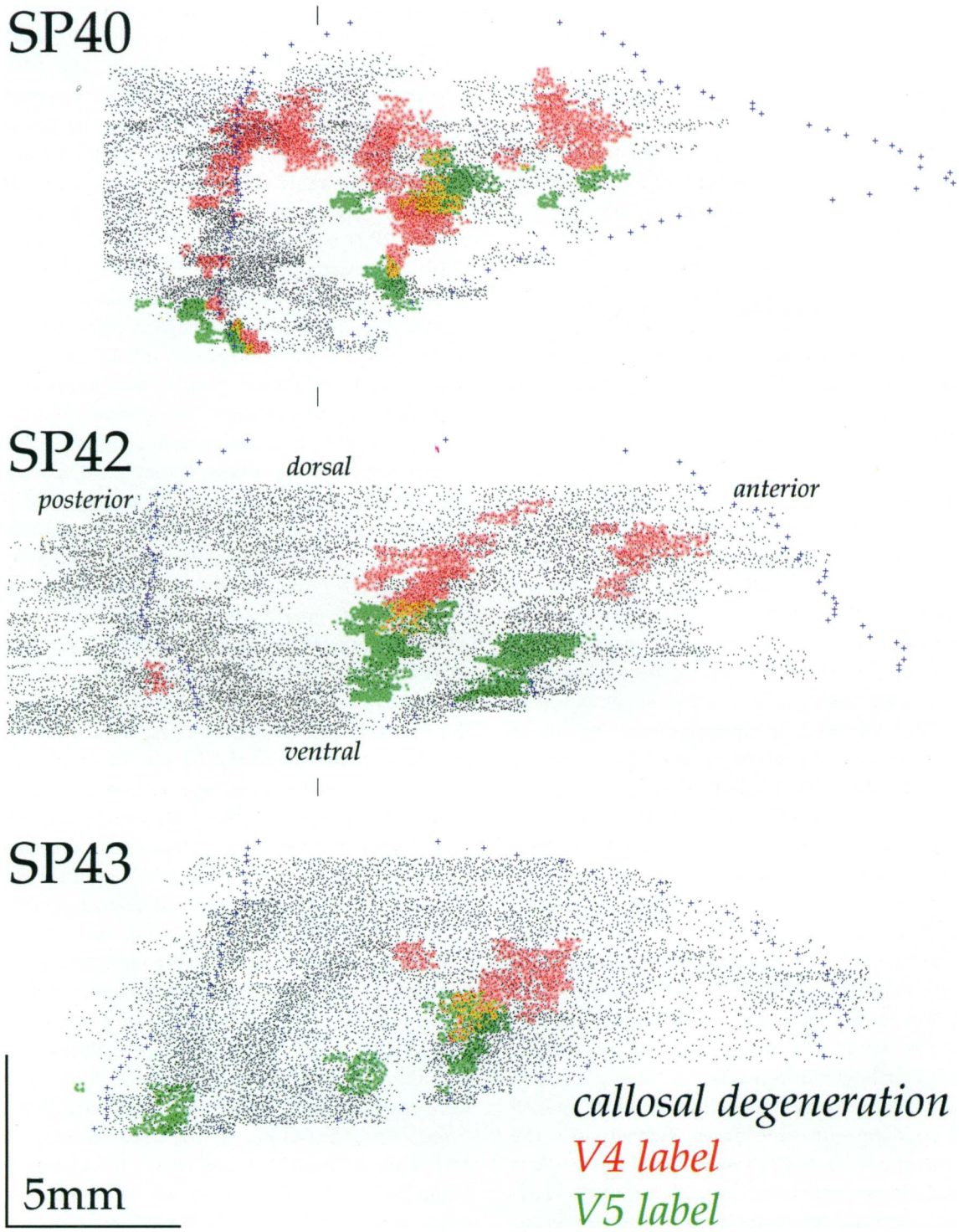

Fig. 8. 2D reconstruction of the distributions of the two tracers, and of callosal axons, within the lateral bank of the intraparietal sulcus (IPS) of each case. The displayed densities represent the presence of labelled terminals through layers 1–4 for WGA-HRP (V4) and TAA (V5) labels, and of degenerating callosal axons in layers 4–6. In this 2D format the layer 4 contours from composite drawings are fully straightened, plotted horizontally, proportionately spaced apart and aligned on the point of maximum curvature inside the IPS (indicated by the vertical fiducial lines). The use of a random dot pattern to display label density masks the presence of individual contours. Posterior is to the left and dorsal to the top. The chain of + symbols at left show the point at which the IPS turns into the LS; symbols at right indicate the turning point onto the lateral surface of the hemisphere or, more ventrally, the junction of the lateral and medial banks of the IPS.

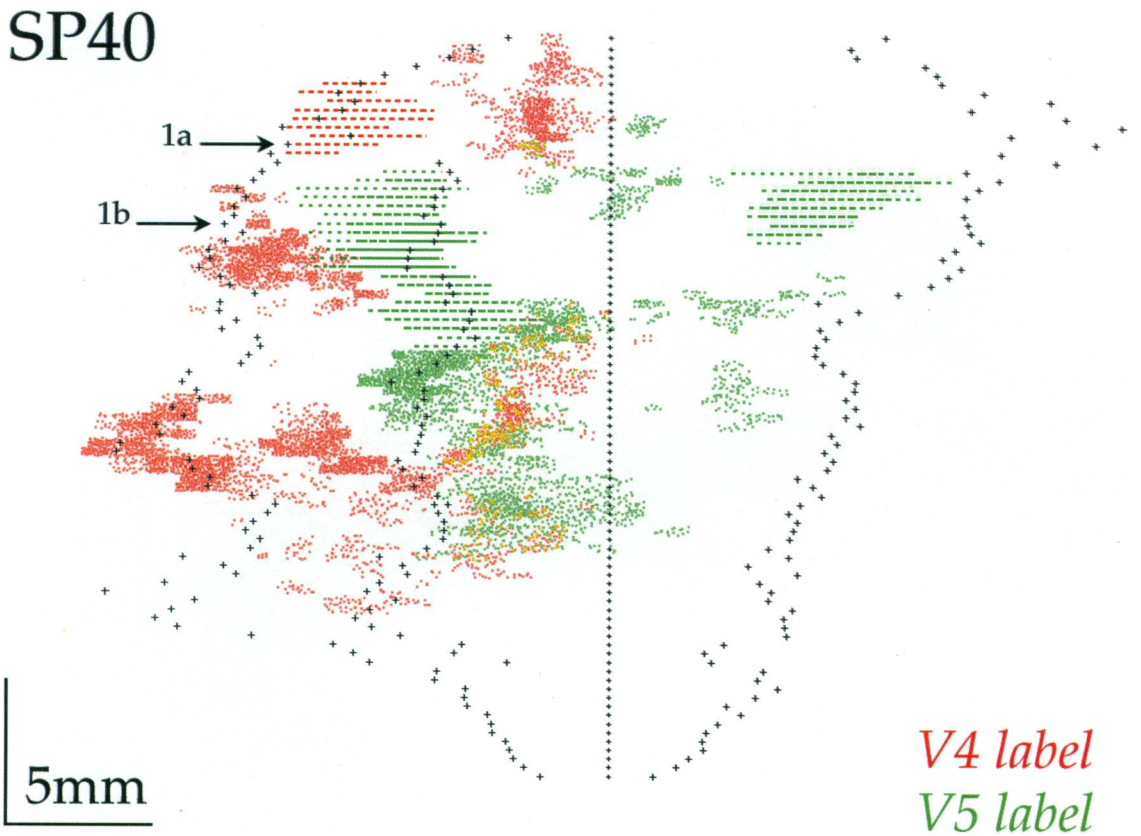

Fig. 9. For legend see page 13.

projection of this type was noted in all 3 cases documented here (and in other unpublished results); if not V4t, this is persistent evidence for a projection from V4 to V5 that is tightly restricted to the lateral margin of V5 alone—an interpretation that seems less plausible given the variable location of V4 injection sites. There was no additional evidence for connections between V4 and V5. Likewise, we did not see a projection from V5 within the territory of V4, although others have reported examples (Maunsell & Van Essen, 1983; Ungerleider & Desimone, 1986). The connections of V4 with more temporal regions of the posterior bank were continuous with those we identified with area TEO in adjacent parts of ITC. However, the most recent definition of TEO is bounded by the lip of the STS (Boussaoud et al. 1991; Distler et al. 1993), so these more temporally located patches of label might alternatively be ascribed to areas PITd or CITd of Van Essen et al. (1990).

Projections from V5 to more dorsal locations in the fundus and anterior bank are likely to represent the connection to area MST, and those to more ventral locations area FST (Maunsell & Van Essen, 1983; Ungerleider & Desimone, 1986). These 2 zones, MST and FST, were the principal sites of STS terminations in 2 cases, but in the third (SP40) the TAA-tracer extended somewhat further towards the temporal pole, possibly exceeding FST to reach into the cortex beyond, which is poorly characterised. There was some light deposition of the TAA tracer in the anterior bank in this case, due to leakage on withdrawal of the injection pipette, which is one possible explanation of the more extensive distribution of projections. A likely projection from V5 to V4t was noted in just 1 case (SP43); if present in the others it may have been sufficiently light to be obscured by the injection halo.

Organisation of connections with the pulvinar

The pulvinar complex contains two major topographic maps, one occupying the inferior pulvinar and part of the lateral pulvinar, the other contained within the lateral pulvinar alone (Bender, 1981; Ungerleider et al. 1983). These maps displayed a rather consistent pattern of connection with V4 and V5, in which there was no overlap between the 2 tracers. Fig. 10 shows adjacent sections from case SP43, where a cluster of V4-tracer is flanked by 2 patches of V5-tracer within the inferior pulvinar. The V4-label is the anterior

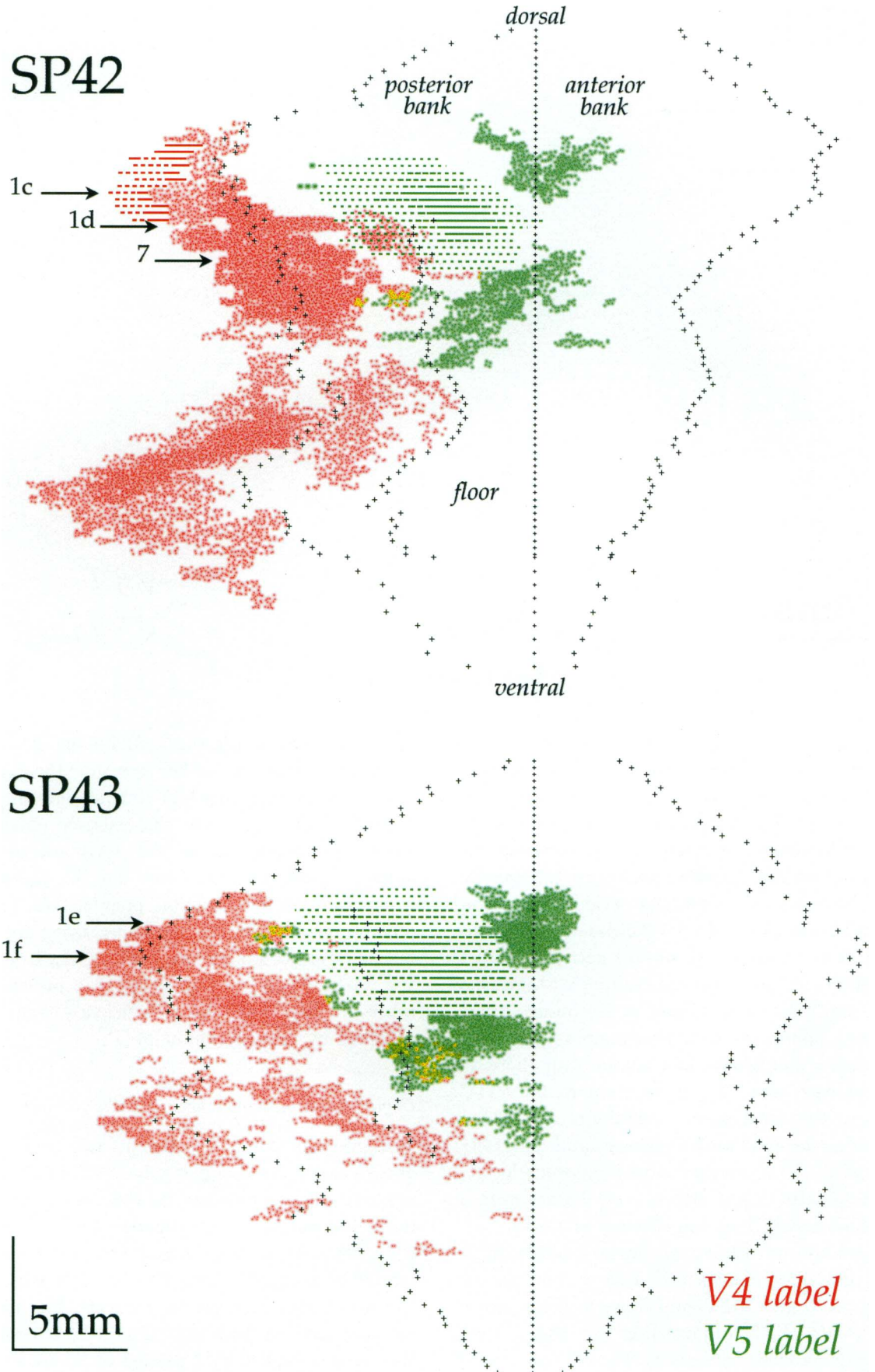

Fig. 9. For legend see opposite.

terminus of a complex distribution seen (in other sections) to extend posteriorly out of the inferior map and back up into the dorsal reaches of the lateral map, representing inferior visual field. The more lateral patch of V5-tracer also lies within the inferior map, at the interface with the LGN. The more medial patch of V5-label lies outside both maps and is part of a crescent-shaped zone reported to connect exclusively with V5 (Standage & Benevento, 1983; Ungerleider et al. 1984). This basic pattern was repeated in each animal described here, and also in many others that we have examined. The V4 tracer, for instance, was never found to extend as far as the interface with the LGN, and the projection of V5 to this site was always compact, in that it never extended very far from this face of the inferior pulvinar.

Of the 3 sites we have described, it is the pulvinar that has the most orderly retinal topography, but there is no simple topographic explanation for our failure to observe direct overlap, either in the pulvinar or elsewhere. This is because the relative location of the V4 and V5 projection domains is fairly consistent between cases—both in the pulvinar and in parietal cortex, for instance—but the topographical relationship between the injection sites in V4 and V5 is not (Fig. 3).

It might, then, be argued that the pulvinar maps cannot be so orderly, given that substantial topographic overlap was demonstrated quite clearly in area V2. However, this is not our interpretation. It should be recalled that the pulvinar is a relatively homogeneous, nonlaminated 3-dimensional structure—unlike the cortex which is a thin, laminar sheet of tissue easily reduced to 2 dimensions for cartographic purposes. A point on the retina maps onto a line through the pulvinar (a line of 'iso-representation'), and it is our assumption that the cortical fields of projection may be separate along this third dimension—in other words that retinotopically equivalent parts of V4 and V5 may connect with different portions of the corresponding, notional, line of iso-representation in the inferior pulvinar. We infer that the lines of iso-representation in the pulvinar are roughly perpendicular to the interface with the LGN. There is evidence for this in Figure 10, since a line drawn from the patch of V4-tracer to the patch of V5-tracer at the LGN interface is roughly perpendicular to this face. Such an arrangement does not quite match the description given by Bender (1981), though it is consistent with the recordings that he illustrates.

DISCUSSION

In principle, major pathways within the cerebral cortex must be defined by mutual exclusion: it is possible to recognise a certain degree of cross-connectivity between 2 otherwise distinct pathways, but when this cross-connectivity exceeds a certain arbitrary level, it makes more sense to refer to a network of connections, in preference to 2 distinct pathways. It was this viewpoint we had in mind in attempting to establish whether the projections of the thin, thick and interstripes of V2 maintain their segregation at higher levels of cortex, or whether these distinctions are dissolved by overlapping convergent connections. Since the ascending projections of areas V4 and V5 that we have studied exhibit only limited instances of direct convergence, and since the reciprocal connections between these two areas are insubstantial or haphazard, we conclude that the pathways deriving from thick stripes (via V5), and from thin and interstripes (via V4), largely preserve their separate identities through at least two subsequent steps of cortical processing.

It is also true, however, that these pathways do not diverge to totally separate cortical regions. On the contrary, both may be traced into both the parietal and temporal lobes, subdivisions of the brain that are often held to incorporate the dorsal 'WHERE' and ventral 'WHAT' pathways respectively (Ungerleider & Mishkin, 1982; Mishkin et al. 1983; Maunsell, 1987; Desimone & Ungerleider, 1989). So the 'two pathway hypothesis' that one might deduce from studying the outputs from V2, and from V4 and V5, is clearly rather different in its nature to the 'two pathway hypothesis' of popular neurology (Newcombe et al. 1987; Haxby et al. 1993). The latter emphasises the difference in function between the dorsal and ventral halves of extrastriate cortex but, given their degree of cross connectivity, it is questionable whether the dichotomy is best described as two distinct 'pathways'. Rather, the anatomically

Fig. 9. 2D reconstructions of the distributions of the two tracers within the superior temporal sulcus in each case, according to the format of Figure 8. Injection sites are shown as unbroken horizontal lines (core) and dashes (halo). The vertical line of symbols indicates the point on which the layer 4 contours were aligned, the fundus or anterior corner of the 'floor' of the sulcus. The chains of + symbols at far left and right show the posterior and anterior lips of the sulcus, respectively. The more central chain of symbols shows the posterior corner of the floor of the sulcus. Dorsal is to the top of each reconstruction. Horizontal arrows indicate the levels of sections illustrated in Figures 1 and 7.

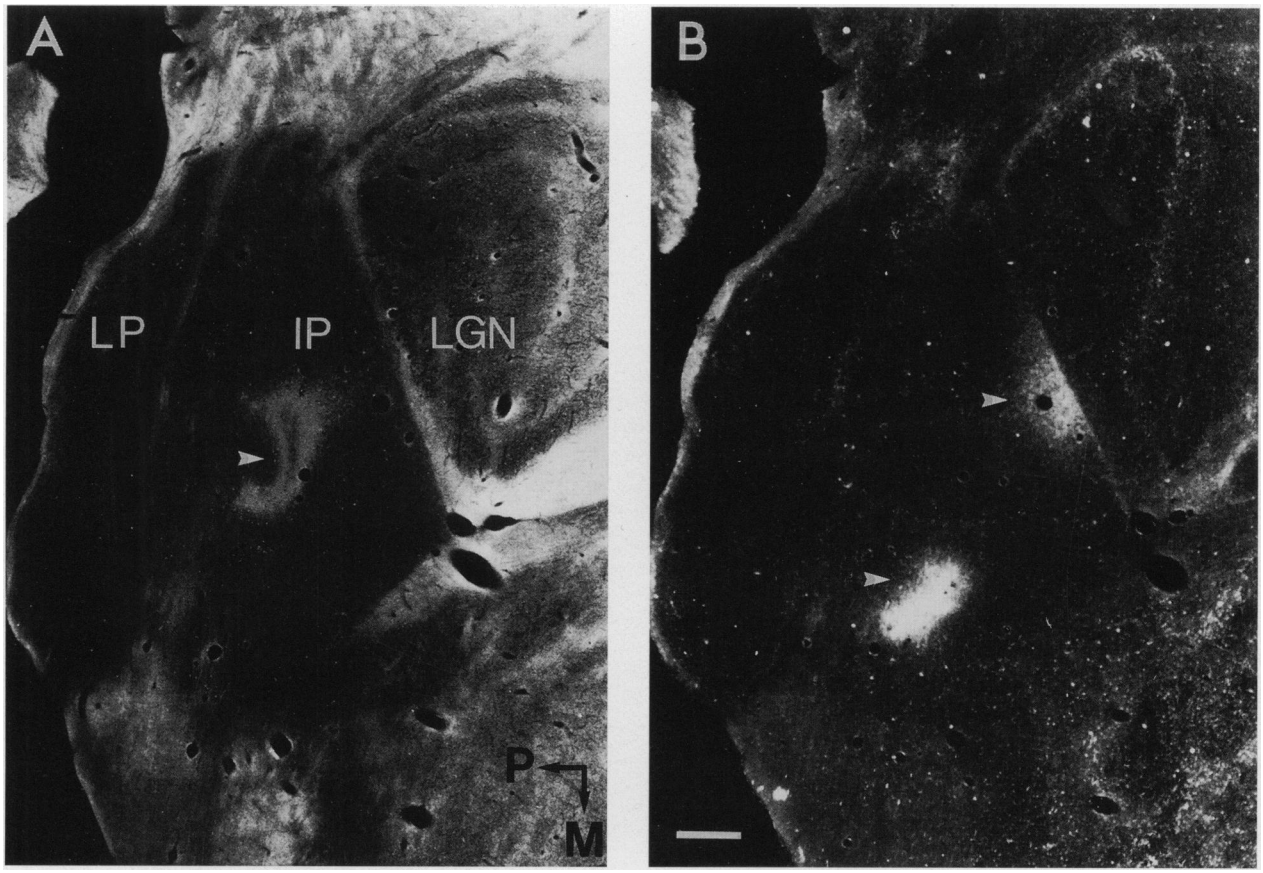

Fig. 10. (A) Horizontal section through the pulvinar and lateral geniculate nucleus showing a cluster of cells and terminals labelled with WGA-HRP following an injection into V4 (case SP43). (B) The adjacent section showing two patches of TAA label derived from V5 (case SP43). Patches of label are earmarked by arrowheads. LP, lateral pulvinar; IP, inferior pulvinar; LGN, lateral geniculate nucleus; M, medial, P, posterior. Bar, 0.5 mm.

distinct pathways out of V2 each appear to branch, and to distribute in parallel to a number of separate but nearby destinations. We refer to this pattern of wiring as 'juxtaconvergence'.

Furthermore, looking at the outputs from V2, we should perhaps identify three pathways, not two. The blob-thin stripe and interblob-interstripe pathways both lead to area V4, but there is anatomical evidence that they remain distinct in this area (Shipp & Zeki, 1985; Zeki & Shipp, 1989; Van Essen et al. 1990). The evidence we present here suggests that these two pathways do not diverge subsequently either, for each projects (via V4) to roughly the same regions of parietal, temporal and frontal cortex; both also connect directly to temporal cortex (area TEO) from V2, bypassing V4 (Nakamura et al. 1993). We cannot tell from our material whether these two pathways recombine at cortical areas beyond V4, or whether in these areas, too, there is some form of modular substructure that preserves the functional identity of the blob-thin stripe and interblob-interstripe pathways at still higher levels. A recent report by DeYoe et al. (1994) suggests that the latter may be the case—although this conclusion is based on injecting retrograde tracers into V4, and thereby revealing the distribution of cells providing feedback to each compartment in V4, rather than revealing the pattern of their ascending afferent distribution.

The principle that functionally distinct pathways may project to juxtaposed regions with minimal overlap is also observed in the subcortical output from V4 and V5 to the pulvinar complex of the thalamus. Even within the single, well ordered, topographic map of the inferior pulvinar, there appear to be separate projection domains of V4 and V5. It is difficult to imagine what purpose could be served by bringing together inputs from two highly dissimilar functional areas, with preservation of their retinotopic order, if all further processing were to remain entirely independent. Anatomical studies which have investigated pulvino-cortical connections by injecting tracing substances into the pulvinar have not commented on the presence of the necessary intrinsic connectivity; on the other hand, the injection sites would have been

large, possibly obscuring local internal transport (Benevento & Rezak, 1976; Ogren & Hendrickson, 1977; Rezak & Benevento, 1979). Local intrinsic connections are an established feature of cortical organisation, so the juxtaconvergence of the cortical pathways is sufficient to bring them within range of each other by local interactions which can extend over several mm (Amir et al. 1993; Lund et al. 1993). We guess that the same principle may hold for the local organisation of the pulvinar. And, more generally, that the continued association of distinct pathways through several stages of cortical and subcortical processing facilitates the mutual exchange of information, for reasons that must promote—rather than blur—their specialised functional roles (Shipp, 1995).

ACKNOWLEDGEMENTS

The authors thank Ian Wilson for histology, John Romaya and Brian Skidmore for brain reconstruction software, and Grant Wray for assistance with graphics. This work was supported by the Wellcome Trust.

REFERENCES

AMIR Y, HAREL M, MALACH R (1993) Cortical hierarchy reflected in the organization of intrinsic connections in macaque visual cortex. *Journal of Comparative Neurology* **334**, 19–46.

ANDERSEN RA, ASANUMA A, ESSICK G, SIEGEL RM (1990) Corticocortical connections of anatomically and physiologically defined subdivisions within the inferior parietal lobule. *Journal of Comparative Neurology* **296**, 65–113.

BENDER DB (1981) Retinotopic organization of macaque pulvinar. *Journal of Neurophysiology* **46**, 672–693.

BENEVENTO LA, REZAK M (1976) The cortical projections of the inferior pulvinar and adjacent lateral pulvinar in the rhesus monkey (Macaca mulatta): an autoradiographic study. *Brain Research* **108**, 1–24.

BLATT, GJ, ANDERSEN RA, STONER GR (1990) Visual receptive field organization and cortico–cortical connections of the lateral intraparietal area (area LIP) in the macaque. *Journal of Comparative Neurology* **299**, 421–445.

BOUSSAOUD D, DESIMONE R, UNGERLEIDER LG (1991) Visual topography of area TEO in the macaque. *Journal of Comparative Neurology* **306**, 554–575.

COLBY CL, DUHAMEL JR, GOLDBERG ME (1993) Ventral intraparietal area of the macaque: anatomic location and visual response properties. *Journal of Neurophysiology* **69**, 902–914.

COWAN WM, GOTTLIEB DI, HENDRICKSON AE, PRICE JL, WOOLSEY TA (1972) The autoradiographic demonstration of axonal connections in the central nervous system. *Brain Research* **37**, 21–51.

DESIMONE R, UNGERLEIDER LG (1986) Multiple visual areas in the caudal superior temporal sulcus of the macaque. *Journal of Comparative Neurology* **248**, 164–189.

DESIMONE R, UNGERLEIDER LG (1989) Neural mechanisms of visual processing in monkeys. In *Handbook of Neuropsychology* (ed. F. Boller & J. Grafman) pp. 267–299. Amsterdam: Elsevier

DEYOE EA, FELLEMAN DJ, VAN ESSEN DC, MCCLENDON E (1994) Multiple processing streams in occipitotemporal visual cortex. *Nature* **371**, 151–154.

DEYOE EA, VAN ESSEN DC (1985) Segregation of efferent connections and receptive field properties in visual area 2 of the macaque. *Nature* **317**, 58–61.

DISTLER C, BOUSSAOUD D, DESIMONE R, UNGERLEIDER LG (1993) Cortical connections of inferior temporal area TEO in macaque monkeys. *Journal of Comparative Neurology* **334**, 125–150.

FELLEMAN DJ, VAN ESSEN DC (1991) Distributed hierarchical processing in the primate cerebral cortex. *Cerebral Cortex* **1**, 1–47.

FINK RP, HEIMER L (1967) Two methods for selective silver impregnation of degenerating axons and their synaptic endings in the central nervous systems. *Brain Research* **4**, 369–374.

GATTASS R, GROSS CG, SANDELL JH (1981) Visual topography of V2 in the macaque. *Journal of Comparative Neurology* **201**, 519–539.

GATTASS R, SOUSA APB, GROSS CG (1988) Visuotopic organization and extent of V3 and V4 of the macaque. *Journal of Neuroscience* **8**, 1831–1845.

HAXBY JV, GRADY CL, HORWITZ B, SALERNO J, UNGERLEIDER LG, MISHKIN M et al. (1993) Dissociation of object and spatial visual processing pathways in human extrastriate cortex. In *Functional Organisation of the Human Visual Cortex*. (ed. B. Gulyas, D. Ottoson & P. Roland) pp. 329–340. Oxford, Pergamon.

HENDRY SHC, YOSHIOKA T (1994) A neurochemically distinct third channel in the macaque dorsal lateral geniculate nucleus. *Science* **264**, 575–577.

LACHICA EA, BECK, P, CASAGRANDE VA (1992) Parallel pathways in macaque monkey striate cortex: anatomically defined columns in layer III. *Proceedings of the National Academy of Sciences of the USA* **89**, 3566–3570.

LIVINGSTONE MS, HUBEL DH (1984) Anatomy and physiology of a color system in the primate visual cortex. *Journal of Neuroscience* **4**, 309–356.

LIVINGSTONE MS, HUBEL DH (1987*a*) Connections between layer 4B of area 17 and the thick cytochrome oxidase stripes of area 18 in the squirrel monkey. *Journal of Neuroscience* **7**, 3371–3377.

LIVINGSTONE MS, HUBEL DH (1987*b*) Psychophysical evidence for separate channels for the perception of form, color, movement, and depth. *Journal of Neuroscience* **7**, 3416–3468.

LUND JS, YOSHIOKA T, LEVITT JB (1993) Comparison of intrinsic connectivity in different areas of macaque monkey cerebral cortex. *Cerebral Cortex* **3**, 148–162.

MAGUIRE WM, BAIZER JS (1984) Visuotopic organization of the prelunate gyrus in rhesus monkey. *Journal of Neuroscience* **4**, 1690–1704.

MAUNSELL JHR (1987) Physiological evidence for two visual subsystems. In *Matters of Intelligence* (ed. L. Vaina) pp. 59–87. Dordrecht: Reidel

MAUNSELL JHR, VAN ESSEN DC (1983) The connections of the middle temporal area and their relationship to a cortical hierarchy in the macaque monkey. *Journal of Neuroscience* **3**, 2563–2586.

MESULAM MM (1982) *Tracing Neural Connections with Horseradish Peroxidase*. New York: Wiley.

MISHKIN M, UNGERLEIDER LG, MACKO KA (1983) Object vision and spatial vision: two cortical pathways. *Trends in Neuroscience* **6**, 414–417.

NAKAMURA M, GATTASS R, DESIMONE R, UNGERLEIDER LG (1993) The modular organization of projections from areas V1 and V2 to areas V4 and TEO in macaques. *Journal of Neuroscience* **13**, 3681–3691.

NEALEY TA, MAUNSELL JHR (1994) Magnocellular and parvocellular contributions to the responses of neurons in macaque striate cortex. *Journal of Neuroscience* **14**, 2069–2079.

NEWCOMBE F, RATCLIFF G, DAMASIO H (1987) Dissociable visual and spatial impairments following right posterior cerebral

lesions: clinical, neuropsychological and anatomical evidence. *Neuropsychologia* **25**, 149–161.

OGREN MP, HENDRICKSON AE (1977) The distribution of pulvinar terminals in visual areas 17 and 18 of the monkey. *Brain Research* **137**, 343–350.

PERRY VH, COWEY A (1984) Retinal ganglion cells that project to the superior colliculus and pretectum in the macaque monkey. *Neuroscience* **12**, 1125–1137.

PERRY, VH, OEHLER R, COWEY A (1984) Retinal ganglion cells that project to the dorsal lateral geniculate nucleus in the Macaque monkey. *Neuroscience* **12**, 1101–1123.

REZAK M, BENEVENTO LA (1979) A comparison of the projections of the dorsal lateral geniculate nucleus, the inferior pulvinar and adjacent lateral pulvinar to primary visual cortex (area 17) in the macaque monkey. *Brain Research* **167**, 19–40.

ROCKLAND KS, PANDYA DN (1979) Laminar origins and terminations of cortical connections of the occipital lobe in the rhesus monkey. *Brain Research* **179**, 3–20.

ROMAYA J, ZEKI S (1985) Rotatable three-dimensional reconstructions of the macaque monkey brain. *Journal of Physiology* **371**, 25P.

SHAPLEY R, PERRY VH (1986) Cat and monkey retinal ganglion cells and their visual functional roles. *Trends in Neuroscience* **9**, 229–235.

SHIPP S (1995) The odd couple. *Current Biology* **5**, 124–128.

SHIPP S, ZEKI S (1985) Segregation of pathways leading from area V2 to areas V4 and V5 of macaque monkey visual cortex. *Nature* **315**, 32–325.

SHIPP S, ZEKI S (1989*a*) The organization of connections between areas V5 and V1 in macaque monkey visual cortex. *European Journal of Neuroscience* **1**, 309–332.

SHIPP S, ZEKI S (1989*b*) The organization of connections between areas V5 and V2 in macaque monkey visual cortex. *European Journal of Neuroscience* **1**, 333–354.

STANDAGE GP, BENEVENTO LA (1983) The organization of connections between the pulvinar and visual area MT in the macaque monkey. *Brain Research* **262**, 288–294.

TOOTELL RBH, SWITKES E, SILVERMAN MS, HAMILTON SL (1988) Functional anatomy of macaque striate cortex. II. Retinotopic organization. *Journal of Neuroscience* **8**, 1531–1568.

UNGERLEIDER LG, MISHKIN M (1982) Two cortical visual systems. In *Analysis of Visual Behaviour* (ed. D. J. Ingle, M. A. Goodale & R. J. W. Mansfield) pp. 549–586. Cambridge, MA: MIT Press.

UNGERLEIDER LG, GALKIN TW, MISHKIN M (1983) Visuotopic organization of projections from striate cortex to inferior and lateral pulvinar in rhesus monkey. *Journal of Comparative Neurology* **217**, 137–157.

UNGERLEIDER LG, DESIMONE R, GALKIN TW, MISHKIN M (1984) Subcortical projections of area MT in the macaque. *Journal of Comparative Neurology* **222**, 368–386.

UNGERLEIDER LG, DESIMONE R (1986) Cortical connections of visual area MT in the macaque. *Journal of Comparative Neurology* **248**, 190–222.

VAN ESSEN DC, FELLEMAN DJ, DEYOE EA, OLAVARRIA J, KNIERIM J (1990) Modular and hierarchical organization of extrastriate visual vortex in the macaque monkey. *Cold Spring Harbor Symposia on Quantitative Biology* **55**, 679–696.

WONG-RILEY MTT (1979) Changes in the visual system of monocularly sutured or enucleated cats demonstrable with cytochrome oxidase histochemistry. *Brain Research* **171**, 11–28.

YOSHIOKA, T, LEVITT JB, LUND JS (1994) Independence and merger of thalamocortical channels within macaque primary visual cortex: anatomy of interlaminar projections. *Visual Neuroscience* **11**, 467–489.

ZEKI SM (1971) Cortical projections from two prestriate areas in the monkey. *Brain Research* **34**, 19–35.

ZEKI S, SHIPP S (1989) Modular connections between areas V2 and V4 of macaque monkey visual cortex. *European Journal of Neuroscience* **1**, 494–506.